Available online at www.sciencedirect.com

ScienceDirect

St. Petersburg Polytechnical University Journal: Physics and Mathematics 1 (2015) 1–8

www.elsevier.com/locate/spjpm

Energetic spectrum and some properties of lead sulfide implanted with oxygen

A.N. Veis

St. Petersburg Polytechnic University, 29 Politekhnicheskaya St., St. Petersburg 195251, Russian Federation

Available online 12 March 2015

Abstract

Spectral dependencies of optical reflection and absorption coefficients in lead sulfide implanted with oxygen ions and annealed in vacuum have been investigated at $T = 300$ K. It was found that the average value of hole concentration within the sample space area where properties were modified by ion implantation and vacuum annealing was equal to $(3.25 \pm 0.30) \times 10^{18}$ cm^{-3}. The depth of the space in question was estimated and its quantity was shown to make the tenths of micrometers. It was demonstrated that because of annealing process oxygen ions occupied places in the chalcogen sublattice healing anion vacancies. It was also found that vacuum annealing of lead sulfide with implanted oxygen did not cause elimination of all anion vacancies. Moreover, the concentration of sulfur vacancies increased considerably in comparison with its value in the initial samples non-subjected to ion implantation. This fact testifies that oxygen in lead sulfide possesses acceptor action which is compensated by chalcogen vacancies. It was established that in the lead sulfide, the only quasi-local energy level, being located in the valence band at the energy distance of 0.16 eV from its top, was connected with oxygen impurity. No other energy level which one could connect with oxygen or with the complexes containing oxygen in lead sulfide was revealed. The storage stability of properties of investigated material was demonstrated.

Keywords: Lead sulfide; Oxygen; Ion implantation; Annealing; Energy spectrum; Conductivity type.

1. Introduction

Lead sulfide (PbS) is widely used in optoelectronics for fabricating infrared radiation sources and detectors. PbS-based light-sensitive cells are, as a rule, *n*-PbS polycrystalline layers grown on glass substrates and annealed in an oxygen-containing environment at 500–550°C. Layer annealing is accompanied by a conductivity inversion from *n*- to *p*-type in near-surface crystalline layers and an occurrence of photosensitivity (see Refs. [1–4] and their respective citations). Even though objects of this type have been studied for more than half a century, the role of oxygen in photoconductivity formation, and its energy spectrum in lead sulfide remain as yet unexplained. This is primarily caused by the complex morphology of oxygen-annealed polycrystalline layers that complicates investigating their properties as well as interpreting the obtained data.

An alternate method of oxygen doping for modifying the properties of lead chalcogenides (and PbS in particular) is currently used besides annealing in an oxygen-containing environment. It is the method of ion implantation combined with post-implantation vacuum

E-mail address: alnveis@mail.ru.

http://dx.doi.org/10.1016/j.spjpm.2015.03.015

(Peer review under responsibility of St. Petersburg Polytechnic University).

annealing of layers for 1–2 h at 250–300°C [5,6]. This is also accompanied by a conductivity inversion from *n*- to *p*-type in near-surface layers of oxygen-implanted films and an occurrence of photosensitivity. It appears that ion implantation may be successfully used as a tool of studying the energy spectrum of oxygen in lead chalcogenides. This problem was solved for lead telluride (PbTe) and lead selenide (PbSe) in Refs. [6,7]. These works also demonstrate that in these materials, oxygen forms a single energy level located deep in the valence band and higher than the anion vacancy level. No other energy level that could be connected to oxygen, or oxygen-containing complexes, was found either in PbTe, or in PbSe.

The authors of Ref. [6] also attempted to obtain experimental data on the properties of oxygen-implanted and vacuum-annealed lead sulfide. They demonstrated that the average hole concentration, $\langle p \rangle$, in PbS : O^+ within the region whose properties had been modified by means of ion implantation and annealing was $(4.0 \pm 0.6) \times 10^{18}$ cm^{-3}, while the oxygen energy level E_O was located deep in the valence band in 0.16 eV from its upper edge (from here onward oxygen ion-implanted and vacuum-annealed samples will be denoted shortly as *n*-PbS : O^+ or *p*-PbS : O^+ with the first letter indicating the conductivity type in the initial non-implanted sample).

These studies have not been concluded and were resumed only 15 years later. They set a number of goals, with the foremost being determining the stability of PbS : O^+ properties over time. For this purpose a repeat study of optical reflectivity (R) spectra in ion-implanted samples was necessary. In case PbS : O^+ properties were indeed proved to be stable, a detailed study of optical absorption spectra α in PbS : O^+ would be worth carrying out to estimate the main parameters of the ion-implanted region, in particular its thickness d^*.

Hereinafter the following notations for the thickness of the examined samples will be used for convenience: d_{st} for an original sample with *p*-type conductivity, d_p and d_n for ion-implanted and annealed samples with *p*- and *n*-type conductivity, respectively.

2. Experimental procedure

2.1. Preparing the samples for examination

The procedure of preparing the samples was briefly described in Ref. [6]. We provide a more detailed description below.

The objects of this study were monocrystalline lead sulfide samples grown using the Bridgman–Stockbarger method and slow cooling from the melt and subjected to homogenized annealing in vacuumed quartz reservoir tubes for a 100 h at 600°C. The monocrystals were doped by either intrinsic crystal lattice defects or a sodium impurity and super-stoichiometric lead (Pb_{ex}).

Free carrier concentrations in studied samples were determined using the Hall method at 78 K. Since considerably large inhomogeneities in the spatial distribution of free carriers are typical for lead sulfide monocrystals, only samples with layer concentrations of free carriers with no more than 3–5% deviation from the Hall values, as determined by optical reflectivity measurements, were chosen for the experiment.

Optical surfaces necessary for examining the reflectivity coefficient spectra were created by mechanically grinding and polishing the samples using the procedure detailed in Ref. [8]. These sample surfaces served as basic and had no further mechanical treatment. These were the surfaces implanted with oxygen using the Vesuvius-1 setup (ion energy was 150 keV, ion-current density was 0.2 μA/cm^2, the dose of implanted oxygen ions was 3000 μC/cm^2, which is equivalent to an oxygen surface concentration $N_0 = 1.87 \times 10^{16}$ cm^{-2}). The doping process was completed by annealing the implanted samples in quartz reservoir tubes (vacuumed to a pressure of 0.13 Pa) for 2 h at 300°C.

Thin samples necessary for recording optical absorption spectra were prepared through grinding their reverse (non-implanted) sides and subsequently making optical surfaces of them according to the procedure described in Ref. [8].

2.2. Measurement procedure

The reflectivity (R) and the transparency (T) coefficients for all samples were measured point by point at room temperature. The number of spectral passes varied from 20 to 30 for R measurements and from 100 to 180 for the T ones. The obtained values of R_i and T_i for each fixed wavelength λ_i were averaged. The scatter of isolated points in the reflectivity coefficient spectra was no more than 1–2%, and that in the transparency coefficient spectra was an order of magnitude less. The $R(\lambda)$ and $T(\lambda)$ dependencies obtained in such a manner were smoothed and used to calculate the absorption coefficient by the formula:

$$\alpha = (1/d)\ln\frac{(1-R)^2 + [(1-R)^4 + 2R^2T^2]^{1/2}}{2T}. \quad (1)$$

The thickness d of the studied samples was measured using a MP-4 microinterferometer with a reliability of $s = 0.90$.

3. Experimental results on light reflection and their discussion

Studying the optical reflectivity spectra of the samples allows to determine the average hole concentration value $\langle p \rangle$ of the ion-implanted region by comparing the data obtained from initial and implanted samples. The first experiment described in Ref. [6] demonstrated that as a result of oxygen ion implantation of samples with subsequent vacuum annealing, the $R(\lambda)$ spectra transformed in different ways. For samples with a low hole concentration in the initial state (p_{st}) the plasma minima λ_{min} in the $R(\lambda)$ spectra shifted toward the short-wave region of the spectrum, and for ones with high p_{st} values the shift was toward the long-wave one. This means that the hole concentration increases after ion implantation and annealing in samples of the first group and decreases in samples of the second group. This observation of the $R(\lambda)$ spectra allowed the authors of Ref. [6] to postulate that the $\langle p \rangle$ value matched the p_{st} hole concentration in those initial samples whose plasma minima did not shift along the energy scale as a result of ion implantation and annealing, and to estimate that value as $(4.0 \pm 0.6) \times 10^{18}$ cm^{-3}.

The present study repeated the examination of the $R(\lambda)$ spectra of all ion-implanted samples, and of some of the initial samples (reverse non-implanted surfaces of massive p-PbS : O^+ crystals were used as initial objects). These examinations allowed to establish that no perceptible changes beyond the experimental error of $\pm$(0.1–0.2) μm occurred in the plasma minimums of all studied samples after 15 years of being kept at room temperature. The data obtained at $R(\lambda)$ spectra registration were supplemented by the thermal EMF coefficient study in thin n-PbS : O^+ crystals (the coefficient was measured by a microprobe). The data analysis demonstrated that conductivity inversion from n- to p-type does indeed occur in samples as a result of ion implantation and vacuum annealing. This means that the PbS : O^+ electrical properties are sufficiently stable with time.

To obtain a more accurate $\langle p \rangle$ estimate than that in Ref. [6], the hole concentration in the initial (p_{st}) and ion-implanted (p_{fin}) samples was calculated for the frequency ω_p of plasma oscillations of free carriers using the formula

$$\omega_p = \left(\frac{4\pi p e^2}{m_R \varepsilon_\infty} \right)^{1/2}. \qquad (2)$$

Here p is the hole concentration, m_R is an effective conductivity mass, and ε_∞ is a high-frequency dielectric permittivity. The values of m_R necessary for calculating p were determined earlier and are shown in Fig. 1.

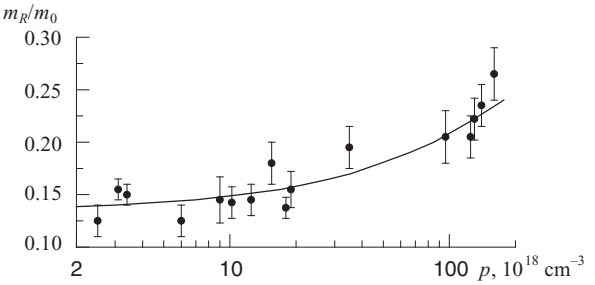

Fig. 1. Experimental (circles) and calculated (line) values of effective conductivity mass m_R vs. the Hall concentration of holes in p-PbS at $T = 300$ K. The calculation according to the Kane model was carried out at a density-of-state effective mass value of 0.27 m_0 in the valence band top.

Indeed, in contrast with the results given in Ref. [6], where finding p_{st} and p_{fin} was based on the earlier obtained $\lambda_{min}(p)$ dependence, which is to say a single point was used in the $R(\lambda)$ spectra of each of the examined samples, while in the present study, ω_p was obtained by calculating the $R(\lambda)$ spectra using the method suggested in Ref. [9]. At the same time we took into account the PbS crystalline lattice contribution to the dielectric function calculated using the data of Ref. [10].

It should be noted that for most of the ion-implanted and vacuum-annealed samples the hole concentration p_{fin}, calculated using (2) does not match the $\langle p \rangle$ value, as the light penetration depth into the sample d_{light}, which can be estimated from the $\alpha d_{light} = 1$ condition, and is found to be equal to about 2–3 μm and which is known to exceed the depth of the d^* layer whose properties have been modified during ion implantation and annealing. This is why we should analyze not the actual p_{fin} and p_{st} values (n_{st} for the case when an electron-type conductivity sample is used as an initial one) but their difference $\Delta p = p_{fin} - p_{st}$ or their sum $\Delta p = p_{fin} + n_{st}$ (n_{st} is the electron concentration in the initial sample). The results of the analysis are shown in Fig. 2. Evidently, the $\Delta p = 0$ condition is fulfilled in lead sulfide for a hole concentration in the initial sample equal to $(3.25 \pm 0.30) \times 10^{18}$ cm^{-3}.

Optical mobilities u_{opt} (at frequencies comparable to ω_p) were also found through calculation of the $R(\lambda)$ spectra. The most interesting data were obtained for p-PbS, wherein

$$p_{st} = (3.5 \pm 0.4) \times 10^{18}\,\text{cm}^{--3} \approx \langle p \rangle .$$

It turned out that for the implanted surface of a massive sample

$$u_{opt} = (405 \pm 20)\ \text{cm}^2/\text{V s},$$

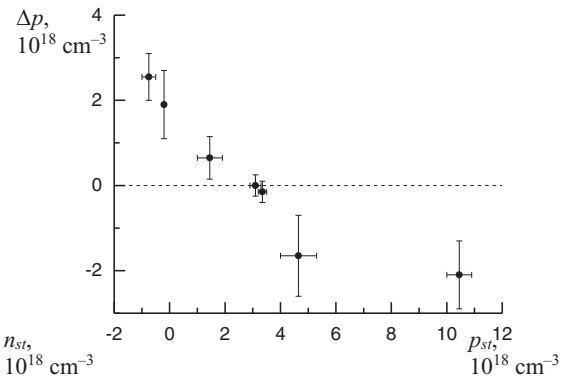

Fig. 2. Plots of the free carrier concentration difference Δp vs. carrier concentration p_{st} and n_{st} in the initial PbS samples.

and for the reverse, non-implanted one

$$u_{opt} = (430 \pm 40)\ \text{cm}^2/\text{V s}.$$

Therefore, in terms of $d_{light} > d^*$, we can assume that the process of ion-doping the lead sulfide with oxygen with subsequent sample annealing does not lead to a fatal decrease in its free hole mobility that could prevent the material from being used in optoelectronics.

4. Experimental results of light absorption and their discussion

Findings of the studied samples to have yielded the most informative results are listed in the table, and their optical absorption spectra are shown in Fig. 3a.

The $\alpha(h\nu)$ dependences depicted are characterized by numerous additional absorption bands related to optical electron transitions to local, quasilocal, and band states. Most of them can be identified by comparing the experimental results (Fig. 3a) within the obtained data set, and to the results given in Refs. [11–14].

The identification is possible as it is experimentally and theoretically proven that all impurity centers in lead chalcogenides are deep [14,15]. Therefore the position of the energy levels they form is determined by the non-Coulomb core part of the impurity potential that is individual for each center. The analysis carried out showed that the α_1 band with a sharp long-wave (red) limit was connected to the complexes whose energy level E_c was located in the lower half of the forbidden band (see Fig. 4 for p-PbS:Na, Pb_{ex} energy schemes corresponding to the experimental data obtained in this study), while the dome-like structure of α_3 was connected to sulfur vacancies forming a quasilocal E_v level

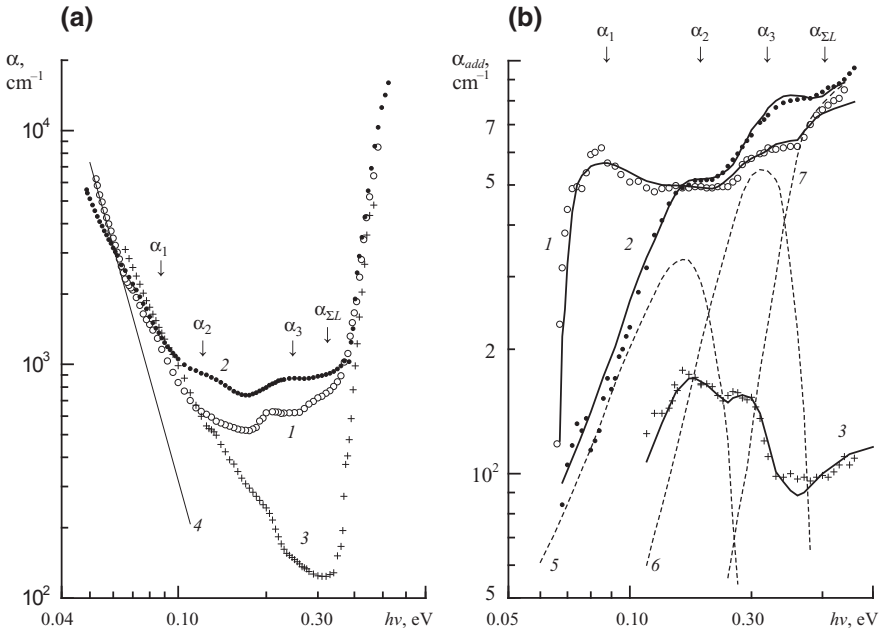

Fig. 3. Experimental (markers) and calculated (lines) absorption coefficient α(a) and additional absorption α_{add} (b) spectra of lead sulfide; $T = 300$ K, sample parameters are listed in the Table 1. *1*, *2*—p-PbS : Na, Pb_{ex} samples, initial, implanted and annealed, respectively, *3*—implanted and annealed n-PbS sample, *4*—linear extrapolation of the free-hole absorption in the initial p-PbS : Na, Pb_{ex} sample; *5–7*—spectral dependences of the α_2, α_3, $\alpha_{\Sigma L}$ components of additional absorption in p-PbS : O^+ calculated using (4) and (5).

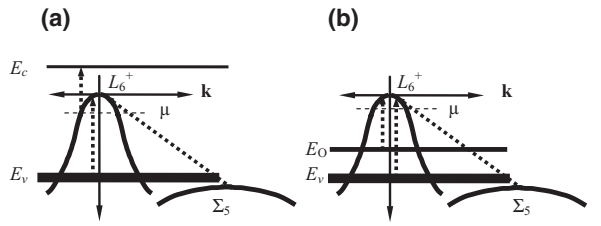

Fig. 4. The energy scheme of the *p*-PbS : Na, Pb_{ex} semiconductor, before (a) and after (b) ion implantation of oxygen and vacuum annealing. Dashed arrows indicate the optical electron transitions observed in the object.

located deep in the valence band, and the $\alpha_{\Sigma L}$ components of the $\alpha(h\nu)$ spectra were connected to optical electron transitions between the Σ_5 and L_6^+ nonequivalent extrema of the valence band.

Only the α_2 bands connected to the optical electron transitions from the E_O quasilocal states, located deep in the valence band, to spreading states near its upper edge do not have any analogies in literature. It should be noted that these bands are present only in the $\alpha(h\nu)$ spectra of the oxygen-implanted and vacuum-annealed samples; that is why the α_2 bands should be attributed to oxygen.

The results of a qualitative analysis of optical spectra were confirmed by the data obtained through calculating the additional absorption frequency dependences $\alpha_{add}(h\nu)$ in studied samples. For this purpose the $\alpha_{add}(h\nu)$ spectra were separated from the $\alpha(h\nu)$ experimental curves by subtracting the α_{fc} absorption of the free charge carriers extrapolated into the shortwave region based on the $\alpha_{fc} \sim (h\nu)^{-n}$ law. The experimental data $\alpha(h\nu)$ are presented in Fig. 3a as a log–log plot, the dependences being straight lines with $-n$ slopes.

This is what allows to linearly extrapolate the free carrier absorption using the experimental dots from the long-wave region of the $\alpha(h\nu)$ spectra. Line 4 in Fig. 3a is an example of such an extrapolation. Note that the n slope values varied within the spread in data for all samples. Some of the data obtained are shown as markers in Fig. 3b.

The calculation of the individual optical absorption spectra components was made using the formulae

$$\alpha_1 = A(h\nu)^{-3}\sqrt{h\nu - E_c^{opt}}, \tag{3}$$

$$\alpha_{2(3)} = B\int_0^\infty E^{1/2}\left[\exp\left(\frac{E-\mu}{kT}\right)+1\right]^{-1} \times \exp\left[-\frac{h\nu - E_{v(O)}^{opt} + E}{2\Gamma_{v(O)}^2}\right] dE, \tag{4}$$

$$\alpha_{\Sigma_L} = C(h\nu)^{-1}\int_u^\infty E^{1/2}(E + h\nu - \Delta E_v)^{1/2} f(E)dE, \tag{5}$$

from Refs. [13,16,17]. In formulae (3)–(5) E_c^{opt} and $E_{v(O)}^{opt}$ are optical ionization energies of centers associated with complexes and sulfur vacancies (an oxygen impurity), respectively; $\Gamma_{v(O)}$ is an energy width of the corresponding quasilocal bands; ΔE_v is an energy gap between nonequivalent valence band extrema; μ is the hole chemical potential; $f(E)$ is the Femi function; A, B and C are proportion coefficients whose values are chosen when adjusting the calculation results to the experimental data.

The results of calculating the individual additional absorption components in an implanted and vacuum-annealed *p*-PbS:Na, Pb_{ex} sample ($p_{st} = (3.5 \pm 0.4) \times 10^{18}$ cm^{-3}, $d_p = (5.20 \pm 0.48)$ μm) are shown in Fig. 3b by the *5–7* curves (in absolute units), and the sums of individual components in each of the studied samples are shown by the *1–3* curves of the same figure. The good agreement between the experimental $\alpha_{add}(h\nu)$ dependences and the calculated curves allowed to determine the energy parameters of the local and quasi-local states found in PbS. These data are listed in Table 1.

The most interesting results from Table 1 are the data for sulfur vacancies (E_v^{opt}) and the intersubband electron transitions in the valence band (ΔE_v) obtained in *p*-PbS : O^+ and *n*-PbS : O^+. The fundamental difference between these samples is that in the first case, the entire bulk of a single crystal exhibits *p*-type conductivity, while in the second case, such a type only extends to a region of d^* width whose properties have been modified through ion implantation and annealing.

Nevertheless, the specified energy parameters of these samples are close to the data obtained from the initial *p*-PbS sample (see Table 1). Notice that the initial sample is also *p*-conductive, so the E_v^{opt} and ΔE_v parameters in the initial and the oxygen-implanted *p*-PbS : Na, Pb_{ex} (shown in Table 1) are unsurprisingly close in value. We can assume that $d_p < d^*$, therefore the contribution of the region with d^* width whose properties have been modified through ion implantation and annealing may not be great. In contrast, the proximity of the E_v^{opt} and ΔE values in *n*-PbS : O^+ and in the initial *p*-PbS is of crucial importance. This gives us reason to suppose that the oxygen volume concentration N_0/d^* in the region of *n*-PbS : O^+ whose properties have been modified through ion implantation and annealing must not be too high.

Table 1
Findings of key parameters of samples studied.

Parameter	Unit	Parameter value			s
		Initial p-PbS	p-PbS : O^+	n-PbS : O^+	
p_{st}, n_{st}	10^{18} cm^{-3}	3.5 ± 0.4	3.5 ± 0.4	0.75 ± 0.25	0.90
p_{fin}	10^{18} cm^{-3}	–	3.2 ± 0.1	1.8 ± 0.3	0.90
d	μm	6.95 ± 0.06	5.20 ± 0.48	15.1 ± 1.6	0.90
E_O^{opt}	eV	–	0.160 ± 0.007	0.165 ± 0.023	0.95
Γ_O^{opt}	eV	–	0.012 ± 0.003	0.009 ± 0.002	0.95
E_v^{opt}	eV	0.238 ± 0.007	0.231 ± 0.009	0.228 ± 0.007	0.95
Γ_v^{opt}	eV	0.027 ± 0.006	0.028 ± 0.005	0.023 ± 0.011	0.95
S_v	cm^{-1} eV	35.5 ± 4.3	53.2 ± 7.6	15.3 ± 1.2	0.90
ΔE_v	eV	0.269 ± 0.012	0.260 ± 0.007	0.258 ± 0.006	0.95
$\alpha_{\Sigma L}^{max}$	cm^{-1}	754 ± 38	919 ± 32	105 ± 20	0.90
E_c^{opt}	eV	0.069 ± 0.001	–	–	0.95
E_g	eV	0.42 ± 0.01	0.43 ± 0,01	–	0.67

The parameter symbols are given in the text; s is the reliability of the parameter found. The E_g values were determined from straight-line cut-offs $\alpha^2(h\nu)$ on the abscissa.

Otherwise the p-conductive region in n-PbS : O^+ should have been regarded as a solid PbS–PbO solution with one of its components, namely, PbO, having a wide energy band gap (according to the data of Ref. [18], the E_g value in PbO is about 2–3 eV). In this case we could have observed a marked decrease in the E_v^{opt} and ΔE_v values in n-PbS : O^+, compared to their values in the initial p-PbS, due to the widening of the band gap in a solid solution.

This, however, does not take place. An insignificant decrease in the E_v^{opt} and ΔE_v values in n-PbS : O^+ compared to the data for the initial sample is within the margin of experimental error and could be regarded merely as a tendency in value decrease of the energy parameters discussed when passing from p-PbS to n-PbS : O^+.

This, in turn, allows us to assume that the volume concentration of oxygen in n-PbS : O^+ must not be higher than 0.5 at. %, or 1×10^{20} cm^{-3}. On one hand, this could be a consequence of the dispersion of the matrix material, and hence of the oxygen implanted into it during ion doping. This phenomenon is discussed in detail in [19,20]. On the other hand, the low N_0/d^* values could be caused by the relatively high d^* values.

The d^* value can be obtained by comparing the intersubband absorption amplitudes $\alpha_{\Sigma_L}^{max}$ in the initial and the ion-doped lead sulfide (values listed in Table 1). It should be taken into account that intersubband electron transitions in the lead chalcogenide valence band are a three-particle process where a third particle, i.e. a phonon or a lattice defect, ensures the quasi-impulse conservation.

This means that the $\alpha_{\Sigma L}$ intersubband coefficients must depend not only on the Hall concentration of holes, but on the number of phonons and crystal lattice defects as well. It also follows from the above that the $\alpha_{\Sigma L}$ values could be different for all three samples listed in Table 1. This makes it impossible to determine the d^* value precisely. A rough estimate of d^* can be obtained only if we assume the imperfection and the size of regions whose properties have been modified through ion doping are the same for p-PbS : O^+ and n-PbS : O^+, while the electrophysical parameters of these regions are homogeneous within their bulk.

Cross-sections of the studied samples explaining the assumptions made are shown in Fig. 5.

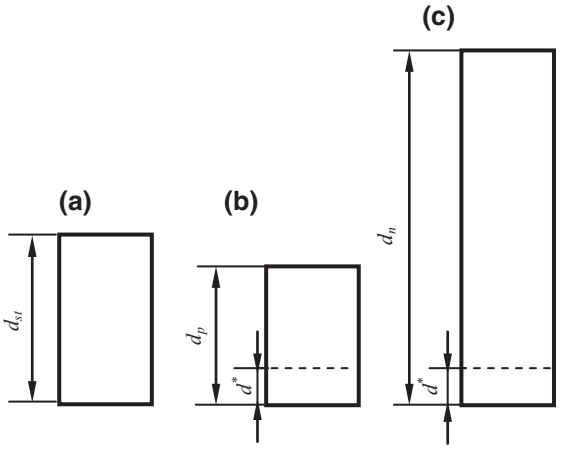

Fig. 5. Cross-sections of the studied samples: the initial p-PbS : Na, Pb_{ex}, $d_{st} = 6.95 \pm 0.06$ μm (a); the same sample, ion-implanted and vacuum-annealed, $d_p = 5.20 \pm 0.48$ μm (b); an ion-implanted and vacuum-annealed n-PbS, $d_n = 15.1 \pm 1.6$ μm (c) (see Table 1).

Accepting these simplifications, d^* value can be estimated using the following simple formula:

$$d^* = \frac{d_p\left(\alpha_{st}^{max} - \alpha_p^{max}\right) + d_n\alpha_n^{max}}{\alpha_{st}^{max}}, \quad (6)$$

where α_{st}^{max}, α_p^{max} and α_n^{max} are the $\alpha_{\Sigma L}$ band amplitudes in the initial p-PbS, p-PbS : O^+ and n-PbS : O^+, respectively.

In accordance with the results of Ref. [21], the error of the d^* parameter (derived from formula (6)) can be estimated using

$$\begin{aligned}(\Delta d^*)^2 = {} & (\Delta d_p)^2\left[1 + \left(\frac{\alpha_p^{max}}{\alpha_{st}^{max}}\right)^2\right] \\ & + (d_p)^2\left[\left(\frac{\Delta\alpha_p^{max}}{\alpha_{st}^{max}}\right)^2 + \frac{\left(\alpha_p^{max}\right)^2}{\left(\alpha_{st}^{max}\right)^4}\left(\Delta\alpha_{st}^{max}\right)^2\right] \\ & + \left(\frac{\alpha_n^{max}}{\alpha_{st}^{max}}\right)^2(\Delta d_n)^2 + (d_n)^2\left[\left(\frac{\Delta\alpha_n^{max}}{\alpha_{st}^{max}}\right)^2\right. \\ & \left. + \frac{\left(\alpha_n^{max}\right)^2}{\left(\alpha_{st}^{max}\right)^4}\left(\Delta\alpha_{st}^{max}\right)^2\right]. \quad (7)\end{aligned}$$

The calculations showed that for studied samples $d^* = (0.96 \pm 0.62)$ μm with a reliability of 0.90. This proves that the not only sample scattering during ion implantation but also the significant depth of the oxygen penetration into the material may contribute to a decrease in the volume concentration of oxygen in an ion-doped lead sulfide.

Let us further discuss the experimental data in Fig. 3a. Comparing these data allows to identify the marked differences in the optical absorption spectra of the initial and the ion-implanted lead sulfides, thus providing insight into the mechanism of the doping effect of oxygen in PbS. Firstly, as a result of ion implantation and annealing, a new quasilocal level E_O, located deep in the valence band, appears in the energy spectrum of lead sulfide that may be bound to oxygen.

No other energy level that could be attributed to either oxygen or to oxygen-containing complexes was found in the energy spectrum of PbS. Moreover, as a result of ion-implanting of the oxygen impurity and the post-implantation annealing of the samples, centers forming the E_c energy level in the band gap of the original p-PbS : Na, Pb_{ex} were destroyed, which the authors of Refs. [11–13] attribute to complexes composed of an acceptor impurity atom (Na or Tl) and a chalcogen vacancy. The elimination of these energy levels as a result of ion doping and annealing of lead sulfide indicates that oxygen atoms occupy positions in the chalcogen sublattice, thus 'healing' the anion vacancies. This, however, does not lead to the elimination of sulfur vacancies in annealed p-PbS : Na, Pb_{ex} doped with oxygen ions. What is more, their number grows, as evidenced by the increase in integral cross-sections of the sulfur vacancy absorption: [formula (8)], transferring from p-PbS to p-PbS:O^+ (A is proportional coefficient)

$$S_v = A\int_0^\infty \alpha_v(h\nu)d(h\nu), \quad (8)$$

This unambiguously proves that oxygen in lead sulfide possesses an acceptor effect compensated by anion vacancies.

5. Summary

The study conducted proved that the properties of oxygen-implanted and vacuum-annealed lead sulfide are sufficiently stable with time. It was demonstrated that oxygen in lead sulfide exhibits acceptor qualities and forms a single energy level located deep in the valence band. It was found that the acceptor effect of oxygen in ion-doped and vacuum-annealed lead sulfide is compensated by sulfur vacancies.

Acknowledgment

The study is supported by the Ministry of Education and Science of the Russian Federation (government grant).

References

[1] Yu.A. Zarif'yants, V.V. Kurylev, Rol' poverkhnostnykh kompleksov v fotochuvstvitel'nosti fizicheskikh sloev PbS (The role of surface complexes in photosensitivity of PbS physical layers), Semiconductors 7 (3) (1973) 598–600.

[2] L.N. Neustroev, V.V. Osipov, K teorii fizicheskikh svojstv fotochuvstvitel'nykh polikristallicheskikh plenok tipa PbS. Fotoprovodimost'. Sravnenie s eksperimentom (On the theory of the physical properties of photosensitive polycrystalline PbS films. Photoconductivity. Comparison with experiment), Semiconductors 20 (1) (1986) 66–71.

[3] A.N. Kovalev, F.I. Manyakhin, Svojstva i mekhanizm fotoprovodimosti polikristallicheskikh sloev sul'fida svintsa (Properties and mechanism of photoconductivity of polycrystalline layers of lead sulfide), Poverkhnost' Fiz. Khim. Mekhan. 2 (1986) 117–126.

[4] A.N. Kovalev, Yu.N. Manyakhin, F.I. Parkhomenko, et al., Profil' raspredeleniya komponentov v pripoverkhnostnom sloe polikristallicheskikh plenok sul'fida svintsa (Distribution of components in the surface layer of polycrystalline films of lead sulfide), Poverkhnost' Fiz. Khim. Mekhan. 11 (1987) 90–95.

[5] Z.M. Dashevskij, L.A. Evmen'ev, V.A. Mazur, et al., Vliyanie ionnoj implantatsii tsinka i kisloroda na svojstva blochno-monokristallicheskikh plenok tellurida svintsa (Effect of ion

implantation of zinc and oxygen on the properties of block-single-crystal films of lead telluride), Tez. dokl. III shkoly po aktual'nym voprosam fiziki polumetallov i uzkozonnykh poluprovodnikov, August 24–30, 1987, Tiraspol', p. 92.

[6] A.N. Veis, Z.M. Dashevskij, M.P. Rulenko, Energeticheskij spektr khal'kogenidov svintsa, implantirovannykh kislorodom (The energy spectrum of lead chalcogenides implanted with oxygen), Neorg. Mater. 28 (12) (1992) 2331–2334.

[7] A.N. Veis, N.A. Suvorova, Energeticheskij spektr selenida svintsa, implantirovannogo kislorodom (The energy spectrum of lead selenide implanted with oxygen), FTP 33 (10) (1999) 1179–1182.

[8] Yu.I. Ukhanov, Optika poluprovodnikov (Semiconductor Optics), vol. 1, Izd. LPI im. M.I. Kalinina, Leningrad, 1970.

[9] A.A. Kukharskij, V.K. Subashiev, Opredelenie nekotorykh parametrov sil'no legirovannykh poluprovodnikov iz spektral'nogo khoda koeffitsienta otrazheniya (Determination of some parameters of heavily doped semiconductors from the spectral variation of the reflection coefficient), FTT 8 (3) (1966) 753–757.

[10] J.R. Dixon, H.R. Riedl, Optical dispersion of lead sulfide in infrared, Phys. Rev. 140 (4A) (1965) 1283–1291.

[11] A.N. Veis, V.I. Kajdanov, R.Yu. Krupitskaya, et al., Osobennosti effekta Kholla i spektrov koeffitsienta pogloshcheniya v sil'no kompensirovannykh obraztsakh khal'kogenidov svintsa (Features of the Hall effect and the spectra of the absorption coefficient in strongly compensated samples of lead chalcogenides), FTP 14 (12) (1980) 2349–2356.

[12] A.N. Veis, R.Yu. Krupitskaya, Primesnye sostoyaniya talliya v sul'fide svintsa po dannym IK-pogloshcheniya (Thallium impurity states in lead sulfide according to the IR absorption), FTP 23 (1) (1989) 185–187.

[13] A.N. Veis, I.M. Leonova, Issledovanie protsessov defektoobrazovaniya v dyrochnom sul'fide svintsa (Investigation of the processes of defect formation in p-type lead sulfide), Trudy SPbGTU 507 (2008) 222–228.

[14] A.N. Veis, Opticheskaya spektroskopiya glubokikh lokal'nykh i kvazilokal'nykh sostoyanij v khal'kogenidakh svintsa (Optical spectroscopy of deep local and quasi-local states in lead chalcogenides), St. Petersburg State Polytech. Univ. J. 2 (54) (2008) 42–51.

[15] V.I. Kajdanov, Yu.I. Ravich, Glubokie i rezonansnye sostoyaniya v poluprovodnikakh tipa $A^{IV}B^{VI}$ (Deep and resonant states in $A^{IV}B^{VI}$ semiconductors), UFN 145 (1) (1985) 55–86.

[16] A.N. Veis, S.A. Nemov, Issledovanie koeffitsienta pogloshcheniya tellurida svintsa, legirovannogo talliem (The study of the absorption coefficient of lead telluride doped with thallium), FTP 13 (12) (1979) 2384–2388.

[17] E. Haga, H. Kimura, Free carrier absorption in III–V semiconductors. IV. Inter-conduction band transitions, J. Phys. Soc. Jpn. 19 (9) (1964) 1596–1606.

[18] V.A. Izvozchikov, O.A. Timofeev, Fotoprovodyashchie okisly svintsa v elektronike, Photoconductive Lead Oxides in Electronics, Energiya, Leningrad, 1979.

[19] N.V. Pleshivtsev, Katodnoe raspylenie, Cathode Sputtering, Atomizdat, Moscow, 1968.

[20] I.A. Abroyan, A.N. Andronov, A.I. Titov, Fizicheskie osnovy elektronnoj i ionnoj tekhnologii (Physical Basis of Electron and Ion Technology), Vysshaya shkola, Moscow, 1984.

[21] A.N. Zajdel', Oshibki izmerenij fizicheskikh velichin (Errors of Measurement of Physical Quantities), Nauka, Leningrad, 1974.